Comparative Study on Directly-Aligned Multi-Point Controlled Wavefront Synthesis and Wave Field Synthesis

Noriyoshi Kamado*, Haruhide Hokari†, Shoji Shimada†, Hiroshi Saruwatari* and Kiyohiro Shikano*
* Nara Institute of Science and Technology, 8916-5 Takayama-cho, Ikoma, Nara 630-0192 Japan
E-mail: noriyoshi-k@is.naist.jp Tel: +81-743-72-5111
† Nagaoka University of Technology, 1603-1 Kamitomioka-machi, Nagaoka, Niigata 940-2188 Japan
E-mail: {hokari,shimada}@vos.nagaokaut.ac.jp Tel/Fax: +81-258-46-6000

***Abstract*—In this paper, we address a comparative study on Directly-Aligned Multi-Point Controlled Wavefront Synthesis (DMCWS) and Wave Field Synthesis (WFS) for realization of high-accuracy sound reproduction system, where amplitude, phase and attenuation characteristics of the wavefronts generated by DWCWS and WFS are assessed. First, in DMCWS, we can derive an optimal control line coordinate based on a numerical analysis. Next, the results of computer simulations reveal that the wavefront of DMCWS has wide availability in both spatial and frequency domains with few amplitude and phase errors, especially beyond the spatial aliasing frequency in WFS. Finally we can point out that the amplitude error of DMCWS has similar behavior to well-known spatial decay approximation expression of WFS; this implies an easiness in handling the amplitude error estimation of DMCWS. From these findings, we can conclude an advantageous position of DMCWS compared with WFS.**

I. Introduction

In recent years, there is an increasing research interest in wavefront synthesis. Wavefront synthesis allows multiple sound sources to create a sound field identical with any original sound field. It is expected to provide a wider effective listening area than that of the current 5.1 or surround system with many channels because the listener can perceive the same sound location regardless of the listening position.

Wavefront synthesis technique has various branches, and typical methods are "Wave Field Synthesis (WFS)" [1] and "Directly-aligned Multi-point Controlled Wavefront Synthesis (DMCWS)" [2], [3]. Although the theory of WFS is well studied, the most optimal control-point geometry and behavior of the secondary wavefront within/beyond the bandlimit in DMCWS are not investigated so far. Hence, in this paper, we describe a DMCWS implementation, and evaluate its effectiveness through the comparison with WFS.

II. Theory

In this section, WFS and MCWS (DMCWS) theories are described, and the concrete numerical calculations are shown in detail.

A. WFS

Geometric configuration and parameters in WFS are depicted in Fig. 1, where $S_P(\omega)$ and $S_{Sn}(\omega)$ denote spectra of the primary and the nth secondary sources, respectively, at X-Y horizontal plane.

The nth secondary source's spectrum which synthesizes the primary spherical wavefront is expressed as [4], [5]

$$S_{Sn}(\omega) = \sqrt{\frac{jk}{2\pi}} C(y_R, y_P) \frac{\exp(-jkr_{Pn})}{\sqrt{r_{Pn}}} \Delta x S_P(\omega) \frac{\cos\theta_{Pn}}{G(\theta_{Pn}, \omega)} \quad (1)$$

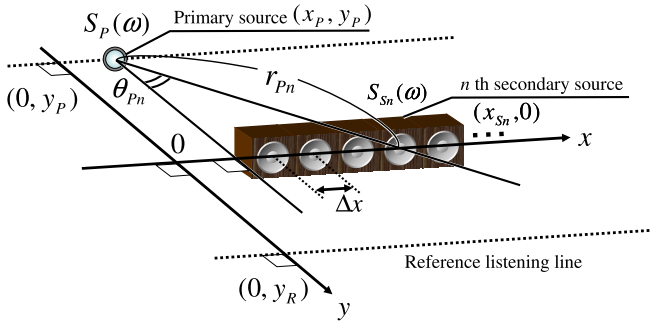

Fig. 1. Configuration of WFS.

where j is unit imaginary number, k is the wavenumber (ω/c), c is the sound velocity, ω denotes the angular frequency, Δx is interelement interval between the secondary sources, r_{Pn} is the distance between primary and the nth secondary source, and θ_{Pn} is the angle between Y axis and the line connecting nth secondary and primary sources. $G(\theta_{Pn}, \omega)$ is a distance-independent directivity function only defined under far-field conditions. $C(y_R, y_P)$ is a function that compensates a level mismatch due to the stationary phase approximation along the x dimension [6], which is only effective at a reference listening distance y_R [7], as

$$C(y_R, y_P) = \sqrt{\frac{|y_R|}{|y_R - y_P|}}. \quad (2)$$

Outside of this line, the level of the sound field is expressed as

$$Att_{S_S}(y) = \sqrt{\frac{|y_R|}{|y|}} \sqrt{\frac{|y| + |y_P|}{|y_R| + |y_P|}} \frac{1}{|y - y_P|}. \quad (3)$$

B. DMCWS

The MCWS's geometric parameters are shown in Fig. 2. MCWS controls the spatial spectra at the control-points located randomly on X-Y horizontal plane in front of secondary sources, and generates desired wavefront. In MCWS, there exists one typical case in that each control-point locates on the control line parallel to x axis cross the position y_C, and its geometric parameters are depicted in Fig. 3 [3]. Such a wavefront synthesis method is called DMCWS (Directly-aligned MCWS) named after its control-point geometry. Here, $S_{Cm}(\omega)$ denotes the secondary wavefront spectrum at the mth control-point position. Also, θ_{Cm} and θ_{Snm} are the angles between Y axis and the line connecting the mth control-point and primary or the nth secondary source, r_{Cm} and r_{Snm} are its spacial distances between the

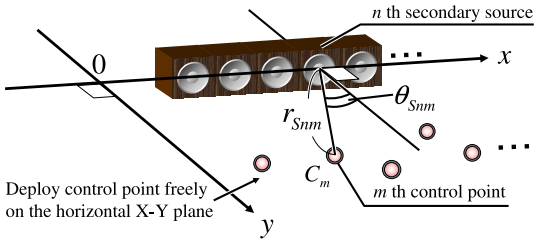

Fig. 2. Configuration of MCWS.

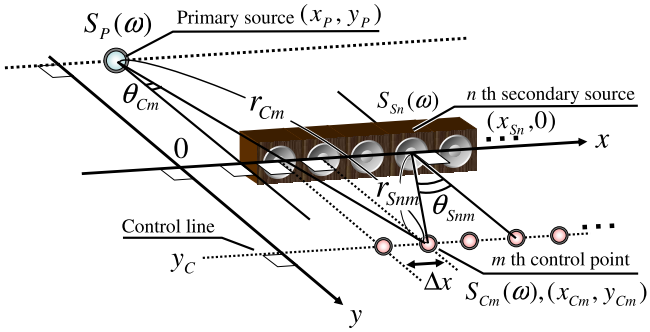

Fig. 3. Configuration for DMCWS.

mth control-point and primary or the nth secondary source, and N and M are the numbers of the secondary sources and the control-points.

Derivation given hereafter is a secondary source's spectrum $S_{Sn}(\omega)$ which synthesizes the primary spherical wavefront. Transfer function between the nth secondary source and the mth control-point, $H_{nm}(\omega)$, is written by

$$H_{nm}(\omega) = G(\theta_{Snm}, \omega)\frac{\exp(-jkr_{Snm})}{r_{Snm}} \tag{4}$$

where $G(\theta, \omega)$ is the directivity characteristics of the secondary sources. According to Eq. (4), we define transfer function matrix

$$\boldsymbol{H}(\omega) = \begin{bmatrix} H_{0,0}(\omega) & H_{1,0}(\omega) & \cdots & H_{N-1,0}(\omega) \\ H_{0,1}(\omega) & H_{1,1}(\omega) & \cdots & H_{N-1,1}(\omega) \\ & \vdots & & \\ H_{0,M-1}(\omega) & H_{1,M-1}(\omega) & \cdots & H_{N-1,M-1}(\omega) \end{bmatrix}. \tag{5}$$

We write secondary wavefront spectrum vector at the mth control-point position as

$$\boldsymbol{S_C}(\omega) = \boldsymbol{H}(\omega)\boldsymbol{S_S}(\omega) \tag{6}$$

where

$$\boldsymbol{S_C}(\omega) = [S_{C0}(\omega), S_{C1}(\omega), \cdots, S_{C(M-1)}]^{\mathrm{T}}, \tag{7}$$

$$\boldsymbol{S_S}(\omega) = [S_{S0}(\omega), S_{S1}(\omega), \cdots, S_{S(N-1)}]^{\mathrm{T}} \tag{8}$$

and $\cdot^{\mathrm{T}}$ denotes transposition of vector/matrix. If the primary wavefront spectrum equals to the secondary wavefront spectrum at the control-point position, Eq. (6) can be transformed into

$$\boldsymbol{S_C}(\omega) = \boldsymbol{P}(\omega)S_P(\omega) \tag{9}$$

where

$$\boldsymbol{P}(\omega) = \left[\frac{e^{-jkr_{C_0}}}{r_{C_0}}, \frac{e^{-jkr_{C_1}}}{r_{C_1}}, \cdots, \frac{e^{-jkr_{C_{M-1}}}}{r_{C_{M-1}}} \right]^{\mathrm{T}}. \tag{10}$$

According to Eqs. (6) and (9), and generalized inverse matrix of $\boldsymbol{H}(\omega)$, $\boldsymbol{H}^{+}(\omega)$, we obtain the secondary source spectrum vector as the following form;

$$\boldsymbol{S_S}(\omega) = \boldsymbol{H}^{+}(\omega)\boldsymbol{P}(\omega)S_P(\omega). \tag{11}$$

TABLE I
WAVEFRONT CALCULATION CONDITION

PARAMETER	VALUE
Temperature	20°C
Evaluated wavefront band frequencies	20~1600 Hz (10 Hz interval)
Spatial aliasing frequency	1416 Hz
Primary source geometry (x_P, y_P)	(1.2,-0.1~-1.0) m
Secondary source and control-point interval Δx	0.12 m
Diaphragm radius b	0.05 m
Number of secondary sources N and control-points M	16
Control line y-coordinate y_C	0.1~2.0 m

Fig. 4. Soundevice SD-0.6 loudspeaker assumed in experiment.

III. Optimized control-point geometry

The DMCWS's secondary wavefront spectrum vector contains the control line geometry, and its optimal geometry has yet to be elucidated fully. Hence we address a study on its geometry through the wavefront calculation in this section.

A. Calculation condition

Conditions of wavefront calculation are shown in Table I. Diaphragm radius b and secondary source distance Δx mimic those of Soundevice SD-0.6 loudspeaker shown in Fig. 4. Evaluated wavefront band frequencies below 1600 Hz are major cues for sound source localization [8]. The wavefront calculation geometric parameters are illustrated in Fig. 5.

B. Calculation method of secondary wavefront

The secondary source and observation point geometric parameters are shown in Fig. 6. Equation (12) represents $S_O(\omega)$ which denotes the spectrum of the secondary wavefront on the observation point,

$$S_O(\omega) = \sum_{n=1}^{N}\left[S_{Sn}(\omega)G(\theta_{On}, \omega)\frac{\exp(-jkr_{On})}{r_{On}}\right]. \tag{12}$$

Secondary sources are circular vibration planes on the infinite baffle and its directional characteristics is

$$G(\theta, \omega) = \frac{2J_1(kb\sin\theta)}{kb\sin\theta} \tag{13}$$

where $J_1(\cdot)$ is Bessel function of the first kind, and b is the diaphragm radius of circular vibration plane.

C. Evaluation criterion of secondary wavefront

$E_{wf}(y_P, y_C)$ defines an evaluation criterion for reproduced wavefront accuracy, as

$$E_{wf}(y_P, y_C) = \frac{\sum^{i,j}\sum^{\omega}\{|\mathrm{CWF}(i,j,\omega)| - |\mathrm{DMCWF}(i,j,\omega)|\}^2}{\sum^{i,j}\sum^{\omega}|\mathrm{CWF}(i,j,\omega)|^2} \tag{14}$$

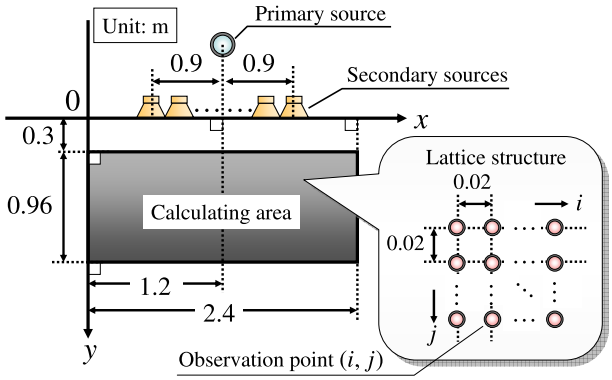

Fig. 5. The wavefront calculation geometric parameters.

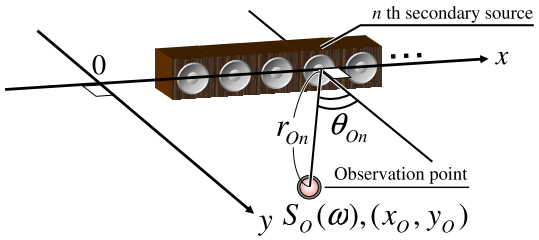

Fig. 6. The secondary source and observation point geometric parameters.

.

TABLE II
CALCULATION CONDITION OF THE DMCWS AND WFS

PARAMETER	VALUE
Primary source geometry	(1.2,-0.1) m
Control line y-coordinate y_C	0.6 m
Reference listening distance y-coordinate y_R	0.6 m

where CWF(i, j, ω) is a function of the primary wavefront spectrum at the observation point (i, j), and DMCWF(i, j, ω) is a function of the DMCWS secondary wavefront spectrum at the same position. Here, $\sum^{\omega}$ and $\sum^{i,j}$ are summations with respect to ω in the evaluation frequency band and observation position (i, j).

D. Calculation results

Figure 7 shows the results for the calculation, where a contour line shows $E_{wf}(y_P, y_C)$ and its interval is 2 dB. Figure 8 shows y_P for the optimized y_C, and its $E_{wf}(y_P, y_C)$ value. The left figure of Fig. 8 shows y_C's best-condition y-coordinates y_{Copt} ranging 0.6 ~ 0.7 m for synthesized secondary wavefront. Also, the right figure of Fig. 8 shows an increase of the evaluation criterion E_{wf} with primary source y-coordinate y_P, and the best-condition y-coordinate y_P under this condition is 0.1 m. Hence, an optimal control line coordinate y_{Copt} is defined as 0.6 m under the primary y-coordinate y_P is 0.1 m. After this, we decide to use these conditions in the computer simulations.

IV. COMPARISON OF DMCWS AND WFS

In this section, we compare DMCWS and WFS through computer-simulation-based experiments on synthesized secondary wavefront spectrum amplitude, phase and attenuation.

A. Calculation condition

The wavefront calculation conditions are listed in Table II, and other conditions are the same as Table I and Fig. 5.

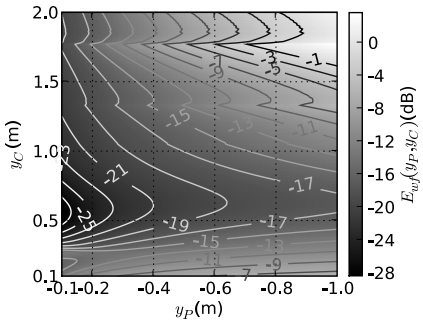

Fig. 7. Contour plot of $E_{wf}(y_P, y_C)$

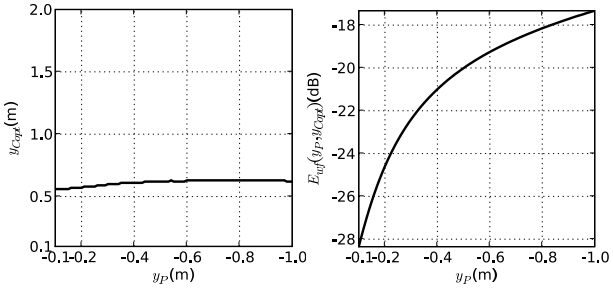

Fig. 8. y_P for the optimized control line y-coordinate y_C and its evaluation value E_{wf}.

B. Evaluation criteria of secondary wavefront

The evaluation criteria E_A and E_P for assessment of secondary wavefront complex amplitude and phase error are defined as

$$E_A(i, j) = \frac{\sum^{\omega} \{|\mathrm{PWF}(i, j, \omega)| - |\mathrm{WF}(i, j, \omega)|\}^2}{\sum^{\omega} |\mathrm{PWF}(i, j, \omega)|^2}, \tag{15}$$

$$E_P(i, j) = \frac{1}{N} \sum^{\omega} \frac{1}{\pi} \arctan\left(\frac{\mathrm{PO}(\mathrm{WF}(i, j, \omega))}{\mathrm{PO}(\mathrm{PWF}(i, j, \omega))} \right) \tag{16}$$

where WF(i, j, ω) denotes secondary wavefront synthesized by DMCWS or WFS, and PO$(\cdot)$ denotes phase only function given by

$$\mathrm{PO}(x) = \frac{x}{|x|} \tag{17}$$

where x is a complex-valued variable.

C. Calculation results

Figures 9 and 10 show WFS's and DMCWS's E_A calculation results. The contour value is E_A, and its intervals are 0.5 dB in Fig. 9 and 2.0 dB in Fig. 10. As can be seen in Fig. 9, the amplitude error of WFS is serious because an evaluation frequency band is beyond spacial aliasing frequency (1417 Hz). In contrast, in Fig. 10, the amplitude error of DMCWS results in 6 – 7 dB, which is small in comparison with WFS as well as generally smallest in the vicinity of a control-point. It is revealed that the difference between the contour lines of Fig. 10 and Fig. 9 yields about 60 dB arround control-points.

Figures 11 and 12 show WFS's and DMCWS's E_P calculation results. The contour value is E_P, and its intervals are 0.05 dB in Fig. 11 and 2.0 dB in Fig. 12. In Fig. 11, the phase error E_P of WFS indicates that there is a significant error similar to the amplitude error in Fig. 9. In contrast, there is an extremely small phase error in DMCWS shown in Fig. 12.

From the above-mentioned results, in the wavefront of DMCWS, an amplitude error was big, but it developed that phase error was small, and consequently the wavefront amplitude error is dominant in DMCWS. Therefore in the next step, we would calculate the attenuation to examine what kind of tendency the wavefront amplitude error

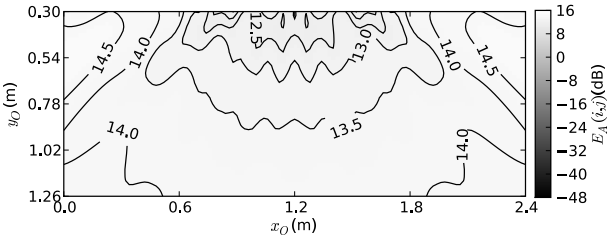

Fig. 9. The amplitude error E_A calculation results of WFS.

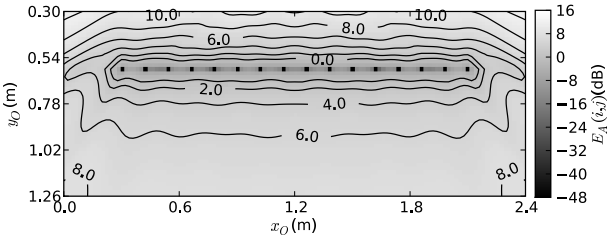

Fig. 10. The amplitude error E_A calculation results of DMCWS.

has. Figures 13 and 14 show comparison of the primary's, WFS's and DMCWS's secondary wavefronts and Att_{S_S} (see Eq. (3)) attenuations in front of the primary source in the upper limit frequency of the evaluation band 1600 Hz. Considering the influence that the primary source y-coordinate y_P gives to wavefront attenuations, we calculate attenuations with y_P of −0.1 m or −0.7 m. Figure 13 shows the result in the case of $y_P = -0.1$ m, Fig. 14 shows that of $y_P = -0.7$ m. The attenuation of WFS is disturbed in comparison to the other attenuation plots greatly in Figs. 13, 14 because the evaluation frequency 1600 Hz is beyond spacial aliasing frequency (1417 Hz). On the other hand, the amplitude of DMCWS has little disorder compared with WFS, and this result suggests a good availability of the wavefront synthesis in frequency bands higher than spacial aliasing frequency. Also, Fig. 14 shows that the attenuation of DMCWS is very close to Att_{S_S} rather than the that of the primary sound source. This result implies a possibility that a Spatial Decay [5] happens in DMCWS in the same way as WFS; this possibly has an easiness in handling the amplitude error estimation of DMCWS.

V. Conclusions

In this paper it is shown that secondary wavefront accuracy is related to the control-point coordinates of DMCWS. Numerical wavefront calculations clarify the optimum directly-aligned control-point coordinates, $y_C = 0.6 \sim 0.7$ m. Also numerical WFS and DMCWS

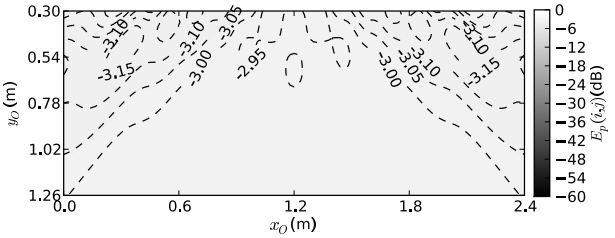

Fig. 11. The phase error E_P calculation results of WFS.

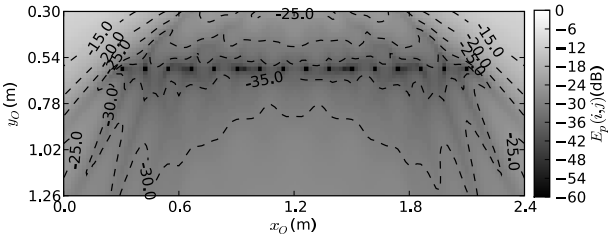

Fig. 12. The phase error E_P calculation results of DMCWS.

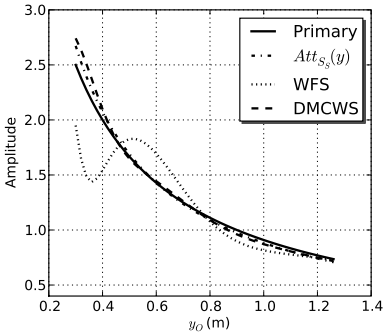

Fig. 13. Comparison of the attenuations in front of the primary source ($y_P = -0.1$ m).

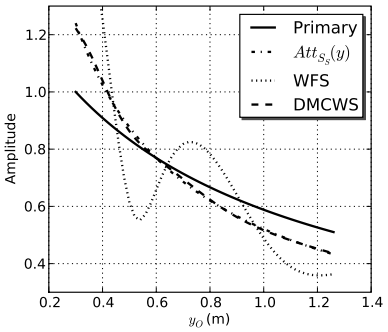

Fig. 14. Comparison of the attenuations in front of the primary source ($y_P = -0.7$ m).

bb

wavefronts compared using these coordinates clarify that DMCWS has larger listening area with a few amplitude and phase errors than those of WFS, while they have similar attenuation error. In addition, DMCWS can realize synthesis beyond the WFS's spatial aliasing frequency. From these findings, we can conclude an advantageous position of DMCWS compared with WFS.

Acknowledgment

This work was partly supported by N·S Promotion Foundation for Science of Perception, and MIC Strategic Information and Communications R&D Promotion Programme in Japan.

References

[1] G. Theile, H. Wittek, K. Ono, K. Hamasaki, "Wave field synthesis : A promising snatial audio rendering concent," The Journal of the Acoustical Society of Japan, Vol.60, No.10, pp.608–613, 2004.

[2] N. Takashima, T. Sugano, S. Uto, H. Harada, "The Basic Study of the Sound Field Control using Multi-channel Adaptive Digital Filters," IEICE Technical report, EA94-38, pp.1–8, 1994.

[3] T. Ohno, H. Hokari, S. Shimada, I. Oohira, " A study on cylindrical wave field synthesis with ultrasmall loudspeaker array," IEICE Technical Report, EA2006-56, pp.7–12, 2006.

[4] D. de Veries, "Sound Reinforcement by Wavefield Synthesis: Adaptation of the Synthesis Operator to the Loudspeaker Directivity Characteristics," J. Audio Eng. Soc., Vol.44, No.12, pp.1120–1131, Dec., 1996.

[5] H. Wittek, "Perception of Spatially Synthesized Sound Fields - Literature Review about WFS," `http://www.hauptmikrofon.de/HW/Wittek_WFS_LitReview.pdf`, Dec. 2003.

[6] E. W. Start, "Direct sound enhancement by wave field synthesis," Ph.D.thesis, Delft University of Technology, Delft, Pays bas, The Netherlands, p.29, 1997.

[7] E. Corteel, "Synthesis of directional sources using wave field synthesis, possibilities, and limitations," EURASIP Journal on Advances in Signal Processing, Vol.2007, Article ID 90509, 2007.

[8] H. Timo, "Two-way acoustic window using wave field synthesis," M. thesis, Helsinki University of Technology, 2007.